Research Article Vol. 13, No. 6 / 1 Jun 2023 / Optical Materials Express 1712
Optical Materials EXPRESS

Challenges in the development of a reliable cw-LIDT measurement routine

KEVIN KIEDROWSKI,[1,*] MARCO JUPÉ,[1,2] HENRIK EHLERS,[3] MICHAEL KENNEDY,[1,2] ANDREAS WIENKE,[1,2] AND DETLEV RISTAU[1,2,4]

[1]*Laser Zentrum Hannover e.V., Optical Components Department, Hollerithallee 8, 30419 Hannover, Germany*
[2]*Cluster of Excellence PhoenixD (Photonics, Optics and Engineering – Innovation Across Disciplines), Welfengarten 1A, 30167 Hannover, Germany*
[3]*Laseroptik GmbH, Horster Straße 20, 30826 Garbsen, Germany*
[4]*Leibniz University Hannover, Institute of Quantum Optics, Welfengarten 1, 30167 Hannover, Germany*
[*]*k.kiedrowski@lzh.de*

Abstract: The characterization of continuous-wave (cw) laser-induced damage threshold (LIDT) requires a suitable measurement routine to obtain reliable results. In this study, we show that the existing measurement protocols are of limited use for cw-LIDT measurements. On the basis of testing several mirrors with varied distance and number of spots on the samples an adapted protocol for the damage behavior under cw laser irradiation is proposed. We observed a significant effect governed by debris and induced stress of induced damages on the damage behavior of subsequent irradiation spots. Finally, we performed a parametric study on the optical properties of mirror designs consisting of a metal and a dielectric multilayer film and demonstrated the LIDT dependence on the thermal conductivity of the substrate and the absorption of the components.

1. Introduction

Many modern laser applications such as laser cutting [1], welding [2,3,4] and laser powder bed fusion [5] require systems with a high average output power. Depending on the application, there are a wide variety of laser concepts in the field. The highest average powers are still achieved by CO_2 laser sources, but there are also numerous lasers available on the market for the near infrared spectral range (NIR), which achieve powers up to hundreds of kilowatts and rising. Further challenges especially for reflective elements arise when they must handle a wide range of angles or spectral areas, for example in opto-mechanical components that experience fast movements, such as in scanners. On the one hand, these components must be very light, on the other hand, the optics must cover a large angular range for different polarizations. In particular, such components require highly complex coatings whose performance stability represents a significant risk for the application. Therefore, for a reliable beam guidance, optical components with high laser damage resistivity are needed. These types of optics often require coatings with a reflective hybrid coating, made of metal thin films and a dielectric multilayer film, deposited for example on a lightweight silicon carbide (SiC) substrate [6]. This ensures precise guidance and positioning of the laser beam as well as keeping the temperature of the component as low as possible to avoid beam distortion.

In general, this means that both, the absorption behavior, which significantly influences the temperature development, and the actual damage threshold are of high interest for the application. In fact, both phenomena are closely linked in continuous laser sources.

In contrast to pulsed irradiation the initial continuous wave (cw) damage mechanism is purely temperature driven. The temperature increases locally during the cw interaction leading to thermal effects due to the absorption in the components. This can lead to laser-induced damage if

#488629 https://doi.org/10.1364/OME.488629
Journal © 2023 Received 23 Feb 2023; revised 28 Apr 2023; accepted 30 Apr 2023; published 22 May 2023

Optical Materials EXPRESS

the temperature and/or temperature gradient reaches a critical value [7,8] preventing the further use of the component by permanent damage or even complete destruction of the optic.

Thus, the phenomenology of destruction appears to be clear and simple to describe, especially because the irradiation time is orders of magnitude greater than the thermal diffusion time of the optical materials involved. Corresponding theoretical approaches are known to the early beginnings of destruction studies [9] and are well developed. However, for a comprehensive investigation of these effects, powerful laser beam sources with high stability and beam quality are required, which, at least in the NIR, have only been available since a few years. Thus, a high number of effects are still poorly understood and researched [10]. In the case of short-pulse applications, it has already been shown [11] that the comparability of measurements and the development of a widely accepted measurement specification are not feasible without an in-depth understanding of the underlying phenomena. Also, for cw testing, there are indications that the damage behavior is not driven purely by intrinsic absorption, but that defects and inhomogeneities play an important role [10]. Consequently, the underlying damage mechanisms are far from being as well understood as expected from the present knowledge based on pure heat conduction models. In addition, there is an increasing demand to significantly expand the data base of the empirical studies, which in turn requires the most appropriate measurement method.

To compare results from different facilities and to perform reliable measurements, a standardized measurement routine is required. Furthermore, the standards need to keep pace with the continuous developments that laser systems and optical components have experienced over the recent decades. For this reason, we performed simulations regarding the temperature increase and temperature gradient due to cw irradiation at different positions on a homogeneous sample without and with cooling of the samples side areas. As sample materials we chose sapphire and fused silica to represent common high-quality substrates to analyze the impact on the heat conduction due to significant differences in the thermal properties. Furthermore, we realized a suitable measurement setup and routine as well as investigated, to what extent laser-induced damages impact the damage behavior of test sites in the vicinity. Applying the obtained results, we adapted the measurement routine to overcome the challenges accompanied by a single laser-induced damage. Furthermore, we used the developed measurement routine to analyze the impact of the absorption of the optical component and the thermal conductivity of the substrate on the LIDT.

2. Simulations

As already indicated in the introduction, damage in the case of continuous irradiation should be initiated mainly through the propagation of heat. An increase in the temperature due to an incident power can be determined by the solution of the heat conduction equation. For a thin infinitely extended optic with uniform absorption this leads to the well-known relation [12]:

$$\Delta T = \frac{\alpha P}{\pi d \rho D C} \text{ for } \tau_{irradiation} \rightarrow \infty \tag{1}$$

With the average laser power P, the absorption α, the beam diameter d, the material density ρ, the heat capacity C and the diffusivity $D = \kappa/\rho C$ with κ the thermal conductivity. Thus, the temperature rise should be proportional to the linear power density P/d and the absorption α in the layer stack.

An optic fulfilling the approximation of a thin and comparatively extended geometry is hardly realized in practice and often accompanied by additional high manufacturing costs. To investigate effects possible during a real LIDT measurement with multiple different irradiation positions on a single sample we simulated the impact of the beam position on the induced temperature increase and maximum temperature gradient. The temperature gradient is proportional to q and κ^{-1}, where q is the conductive heat flux. Moreover, to resemble the test conditions in the measurement setup presented in the experimental section we made approximations and chose

Optical Materials EXPRESS

the parameters, materials, as well as the test conditions in the simulations in accordance with the experiments. We analyzed the temperature increase under cw irradiation for a fused silica and a sapphire substrate (25 mm × 1 mm) with an absorbing surface to estimate the temperature increase in dependence on the beam displacement relative to the optics center. We chose sapphire and fused silica as materials, because these are common high quality substrate materials with relatively high and low thermal conductivity, and to compare the results with our experimental data.

We performed 3D-simulations with the "Heat Transfer Module" in the COMSOL Multiphysics software [13] with the relevant parameters listed in Table 1. The heat losses due to surface-to-surface radiation with an emissivity of 0.95 and due to free convection assuming a value of 10 W/m^{2}K were set to be simulated on all the samples surfaces. The simulation for each data point started with the software's predefined "extremely fine" mesh setting creating elements with sizes between 5.08E-4 m and 5.08E-6 m. During the simulations the "mesh adaptions and error estimates" option was used considering the beam position to further optimize the mesh until the calculated maximum temperature between the last steps showed no significant change. The simulation was set up so that the component completely absorbs the incident power of a Gaussian beam with a 1/e^2-diameter of 200 µm at the surface at an angle of 45°. The beam diameter was chosen to resemble our test conditions in the experimental section.

Table 1. Parameters and settings used in the COMSOL Multiphysics simulations

General settings		Sample property	Sapphire	Fused silica
Substrate diameter	25.4 mm	Heat capacity J/(kg·K)	757 @ 17 °C, 1033 @ 220 °C [14,15]	772 @ 100 °C, 964 @ 500 °C [17]
Substrate thickness	1 mm			
Beam diameter (1/e^2 of the major axis)	282.8 µm			
AOI	45°			
Dimensions	3	Density kg/m^3	3900	2203
Convection	10 W/(m^2·K)			
Emissivity	0.95	Thermal conductivity W/(m·K)	41 @ 0 °C, 20 @ 220 °C [16]	1.38 @ 20 °C, 1.46 @100 °C, 1.55 @ 200 °C [17]
Ambient temperature	20 °C			

The surface was chosen to absorb 100% of the incident power to approximate the thermal behavior due to absorption governed by the coating which is negligibly thin compared to the substrate. Moreover, the absorbed power was chosen to induce a maximum increase of approximately 200 K in the center of the component for both samples, because previous tests, i.e., our own experience and the results of the SPIE Laser Damage Competition [18] showed that the test mirrors are usually damaged at temperature increases of several hundred Kelvins. An illustration of the temperature distribution is exemplarily shown in Fig. 1 for a centered irradiation and a beam displacement of 10 mm relative to the optics center.

Furthermore, we investigated the effect of a cooling unit to estimate if the impact of the beam position on the temperature increase can be adapted to ensure similar conditions for different spots. The cooling was realized by keeping the temperature of the substrate side areas fixed to the ambient temperature to simulate a cooling process appropriate for reflective and transmissive optical components. Apart from this, the simulation was conducted analog to the uncooled investigation. It is important to note that due to the initial approach of a completely absorbing surface the temperature increase is relatively high despite the small incident power. To induce a similar temperature increase in an optic with only 100 ppm absorption a power in the kilowatt range would be required.

Optical Materials EXPRESS

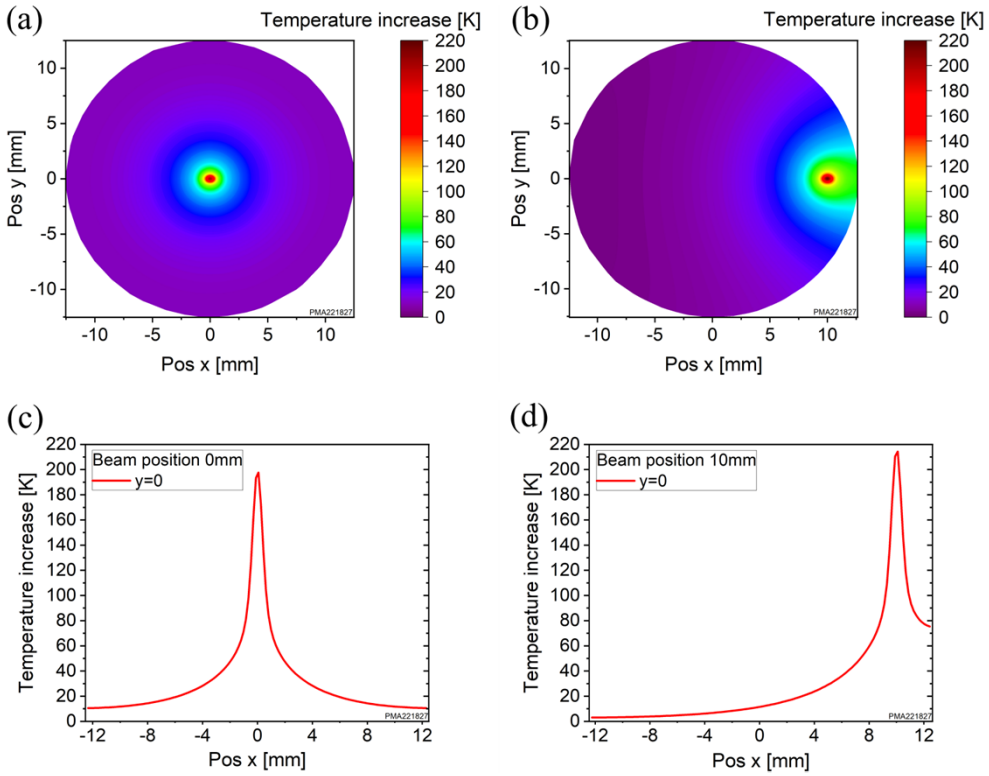

Fig. 1. Simulated equilibrium temperature distribution on the absorbing surface of a free standing fused silica substrate due to a centered irradiation (a) and a displacement of the beam of 10 mm relative to the optics center (b) with an absorbed power of 0.41W. The bottom images (c) and (d) show the corresponding temperature increase in a line on the surface for y = 0 in relation to the images at the top.

The simulation results regarding the beam displacement with and without an external cooling are plotted in Fig. 2. Due to the larger thermal conductivity, the sapphire substrate conducts the heat in a larger area of the component and consequently, the power necessary to induce a temperature increase identical to that in fused silica is 7.6 times higher. Our simulations for the free standing substrates show an increase in the temperature of 6.5% for sapphire and 3.8% for fused silica substrates when the beam is shifted 8 mm from the center position of the sample. For even larger distances the temperature increases even more and the difference between the thermal conductivity of fused silica and sapphire becomes significant. The reason for this general behavior is the reduced volume closer to the edge of the optic, in which the heat can be dissipated to, and the reflection of the heat flux at the edge. Due to the higher heat conductivity value of sapphire, the temperature increase is already noticeable at small shifts of the beam position. However, the low heat conductivity of fused silica leads to a steeper temperature increase close to the samples edge. Even though the maximum temperature increase is the same in the center of the objects, the temperature gradient on the fused silica surface is a factor 1.8 higher than that of sapphire. To achieve a similar temperature gradient in a fused silica substrate the incident power needs to be lowered by a factor of 1.9.

Comparing the maximum temperature increase in the center of the free standing and cooled substrates, the simulations indicate a clear impact of the thermal conductivity. According to the high thermal conductivity of sapphire, the center temperature is reduced from 200 K to

Optical Materials EXPRESS

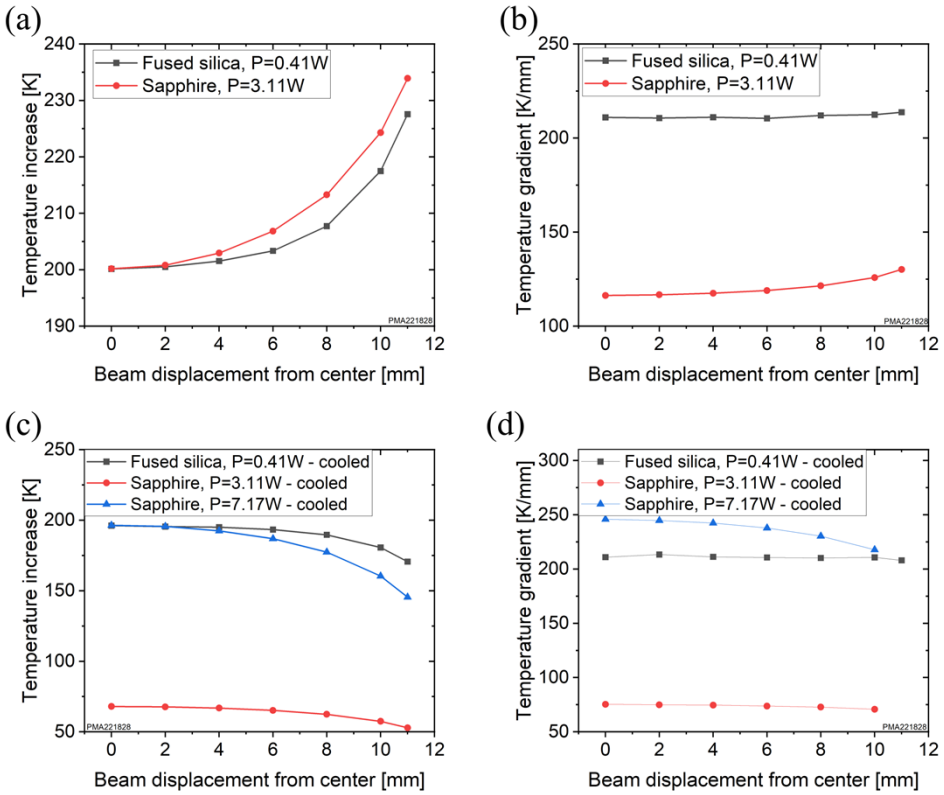

Fig. 2. Simulated maximum temperature increase (a) due to 100% absorption at the surface of a free standing sapphire (black curve) and a fused silica substrate (red curve) in dependence on the beam position on the surface relative to the components center and the simulated maximal temperature gradient (b) in the equilibrium. The corresponding simulations with an external cooling i.e., the substrates side areas temperature fixed to the ambient temperature regarding the maximum temperature increase (c) and the temperature gradient (d).

68 K with cooling. In contrast, the maximum temperature of fused silica is only reduced by approximately 4 K to 196 K due to the significantly lower thermal conductivity. Moreover, as noticeable in Fig. 2(c), the incident power on the cooled sapphire sample (blue curve) can be 17.5 times higher compared to the cooled fused silica substrate (black curve) to achieve the same maximum temperature increase at the center position. However, due to the cooling the maximum temperature increase reduces the closer the beam moves to the edge of the sample, and also the behavior of the maximum temperature varies. The reason for this is the smaller distance between the heat source and the heat sink. Additionally, the temperature gradient seen in Fig. 2 (d) also indicates that a cooling of the samples leads to a rather unpredictable behavior which strongly depends on the substrate's properties. These simulations show that an implementation of a cooling unit for a standardized cw-LIDT measurement is in general difficult to predict because the effect varies a lot depending on the thermal conductivity of different substrate materials, thus the sample of interest shall be tested in an arrangement according to the intended application.

Overall, these results show that the beam position significantly influences the maximum induced temperature increase and temperature gradient during cw irradiation. Regarding an optic with a diameter of 25 mm, a displacement of the irradiation spot by up to 8 mm relative to the center is realistic during LIDT-tests. In case of a damage mechanism governed by a critical

Optical Materials EXPRESS

temperature, this can influence the damage behavior at identical input powers and needs to be considered in the realization of a reliable measurement routine.

The simulation of a sample without a cooling unit already shows that, even with uniform absorption over the whole surface, the damage threshold in the edge region is lower than in the center. Whereas a cooled sample shows the opposite behavior. In addition, there is a clear dependence on the thermal contact and the thermal conduction properties of the substrates. For the application, this means that a proportion of the measurement error will be led back to the thermal properties of the sample and the mounting.

3. Measurement setup

To determine the laser-induced damage threshold (LIDT) we developed and realized a suitable measurement setup, which is depicted in Fig. 3. The circular polarized beam of a commercial thin disk laser with a wavelength of 1030 nm and power up to 6 kW was guided to the setup using a fiber with a 200 µm core diameter, collimated and afterwards focused with a lens with a focal length of 200 mm. A mirror reflecting 87.5% at p- and s-polarized radiation was used to lower the available average power on the sample position as the laser operated stable only at higher output powers. We placed the sample under test parallel to the optical table in a non-fixing mount to avoid influences of clamping mechanisms. Moreover, the angle between the incident beam and the sample was 45°, and the reflected and transmitted beams were terminated by a water-cooled beam trap.

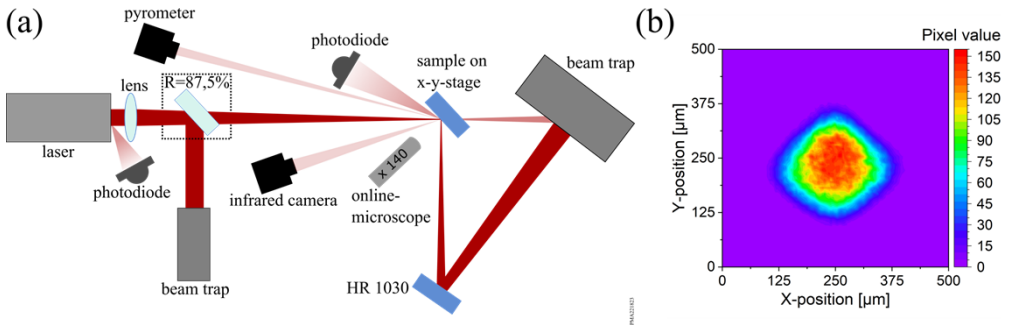

Fig. 3. Measurement setup to determine the laser-induced damage threshold of several mirrors (a) and the beam profile in the focal plane under an angle of incidence of 0° (b).

A photodiode calibrated with the power meter 10K-W-BB-45 from Ophir is directed towards the beam collimator monitoring the power fluctuations of the laser system. For damage detection, light scattered from the surface under test is detected by a second photodiode in the vicinity of the optic. Moreover, the relative temperature change of the sample surface is monitored by the pyrometer KTR 2100-1-L from Maurer and the infrared camera 2126-S309SP-ND from Seek Thermal is used to observe the temperature distribution. A high-resolution online microscope is implemented to examine the irradiation spot regarding impurities on the samples surface.

The beam profile in the beam focus was measured with a CCD-camera at an angle of incidence of 0° and showed a super Gaussian profile. The effective beam diameter at an angle of 0° was 181 µm leading to an effective beam diameter of 256 µm at an angle of 45° in the longer axis. For the calculation of the linear power density at an angle of incidence of 45°, a conservative approach was taken, therefore the length of the longer axis was used. The beam size was chosen due to limitations of the laser device to achieve a sufficient power density to damage the optic.

The mount for the test optics plays a significantly greater role for the investigations in the cw range than for investigations involving short pulse laser radiation. The reason for this is the significant heating of the samples during laser irradiation. On the one hand, the mounting can

Optical Materials EXPRESS

increase the thermally induced stress and thus leading to a lower damage threshold. On the other hand, a properly designed fixture can actively dissipate heat, which is quite common for optical components in high-power operation, and thus actively counteract the destruction. For this reason, water-cooled mirrors for high-power applications commercially exist. For the measurements presented in this study, a support was chosen that exerts mechanical force on the sample and dissipates heat only marginally. This arrangement was initially chosen to create the most universal conditions possible. In practical applications, sometimes very complex cooling systems are used, which, are difficult to reproduce in a standardized measurement without examining the setup as a complete unit.

4. Damage behavior in the cw regime

A prerequisite for a reliable measurement is the independence of each measurement spot on an optic from the others. In view of the morphologies, which will be analyzed in more detail below, this criterion seems to be very decisive for the measurements with high average powers. Thus, our first experiments showed a possible influence of laser-induced damage on the subsequent measurement position of the same test optics. After the first damaged spot appeared, the subsequent damage probability seemed to be higher than one would expect leading to an accumulation of damaged spots in its vicinity at low power densities. Regarding this, the investigations using differential interference contrast (DIC) microscopy showed contamination in a large area up to 5 mm distant to the damage. These contaminations have the sizes of a few micrometers wide and in some cases several hundred micrometer long (Fig. 4). Most likely, it is molten material that is ejected from the destruction area and then cools down. Thus, it is to be expected that not only the material itself forms defects relevant to destruction, but also the surrounding is damaged by the heat-affected zone and contaminations created by the laser induced damages. For this reason, a more detailed investigation regarding the damage zones and the required distance between the measuring positions is necessary.

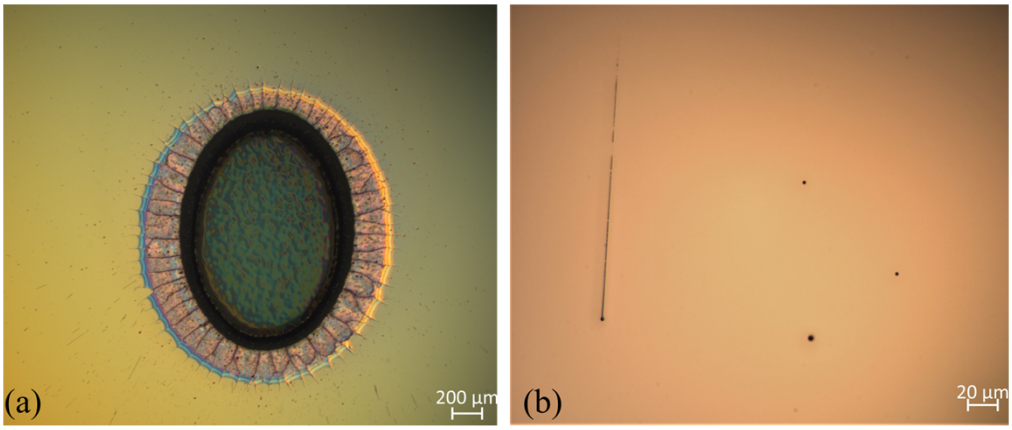

Fig. 4. Laser-induced damage on a fused silica substrate coated with a high reflective dielectric multilayer (a) and the debris in a distance of approximately 5 mm to the laser-induced damage center (b).

Initially, the mirror was placed on a mechanical mount, irradiated at low linear power density (14 kW/cm) for 30 s and then passively cooled down for 90 s. Afterwards, the next site was irradiated. This was repeated until each position was irradiated once with the set power density. Then, the power density was increased, and the same positions were irradiated again. The irradiation was automatically stopped when a damage was detected via increased scattering. This

Optical Materials EXPRESS

process was performed until each position was damaged or the maximum output power of the laser system was reached.

Overall, 16 dielectric mirrors with an HR coating at 1030 nm from the same batch were used in this investigation, manufactured by an electron beam evaporation process using fused silica substrates and a combination of Nb_2O_5 and SiO_2 as the multilayer stack materials. In Table 2, the number of sites for each mirror, the minimal distance between the sites as well as the number of mirrors for each test series is listed.

Table 2. Number of sites, minimal distance between the sites and the number of samples for each test series. (*Only a displacement of 120 µm was done between the power densities)

Number of sites	Minimal distance between sites [mm]	Number of mirrors	Total number of irradiated sites
1	Irradiation near the center*	7	7
4	7.5	5	20
7	5.0	2	14
17	3.5	2	34

Due to the limited number of samples, the statistical certainty is rather small. Therefore, we used a cumulative approach to calculate the damage probability for each test series based on a method proposed by Schrameyer et al. [19]. In this approach, we assume that a site damaged at the power density Pd_i would also been damaged at arbitrary higher power densities $Pd_n > Pd_i$. Moreover, regarding the calculation of the cumulative damage probability we take into consideration the damaged sites of each optic within the same test series e.g., all 20 positions in case of five mirrors with each four irradiated positions. The resulting cumulative damage probabilities are shown in Fig. 5 for the different number of test sites mentioned in Table 2.

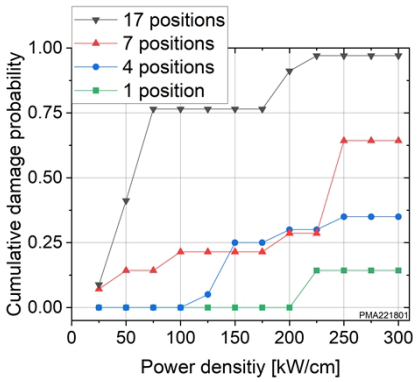

Fig. 5. Cumulative damage probability versus power density depending on the number of sites per sample.

Apparently, the more positions are irradiated on a sample the more likely a damage will occur during the tests, which is why we observed damages at lower power densities for 17 and 7 positions and none for four and one position(s). However, compared to all test series the high increase in the damage probability for low power densities in case of 17 positions is striking high. In case of the pure dielectric mirrors investigated in our studies these results indicate that the overall damage behavior is induced by defects, impurities and/or inhomogeneities of the mirror. In dependence of the irradiated area, i.e. number of positions, the damage onset varies strongly, which leads to an under- or overrated LIDT. Moreover, the figure also indicates that a single

Optical Materials EXPRESS

laser-induced damage position will lower the LIDT of subsequent positions in the vicinity. This is the reason of the rapid increase in the damage probability regarding 17 positions compared to test series with less sites on each optic. This decrease in the LIDT might be due to damages in the coating and the substrate as well as debris and/or thermal induced stress as explained below.

Looking at the measurements with a reduced number of measuring positions, a clear trend can still be observed, which also suggests an interaction of the measuring positions with a significantly increased distance.

Following the LIDT tests, the damaged optics were investigated using DIC microscopy and an in-house developed setup to determine the local scattering of optics [20]. The damages induced by the cw irradiation in this section vary in size depending on the damaging power density. At low power (100 kW/cm) the damaged sizes are in the range of 1-2 mm and reach diameters of up to 5-6 mm for higher power densities (>>100 kW/cm). A typical microscope image and the corresponding scatter image are exemplarily shown in Fig. 6. The bigger crater visible in the microscope image is the initial damage and the second one probably occurs due to a following reflection at the substrates rear surface. In some cases, depending on the power at which the damage occurs, either only the initial damage or an arbitrary formed bigger damage with an even larger impact is observed.

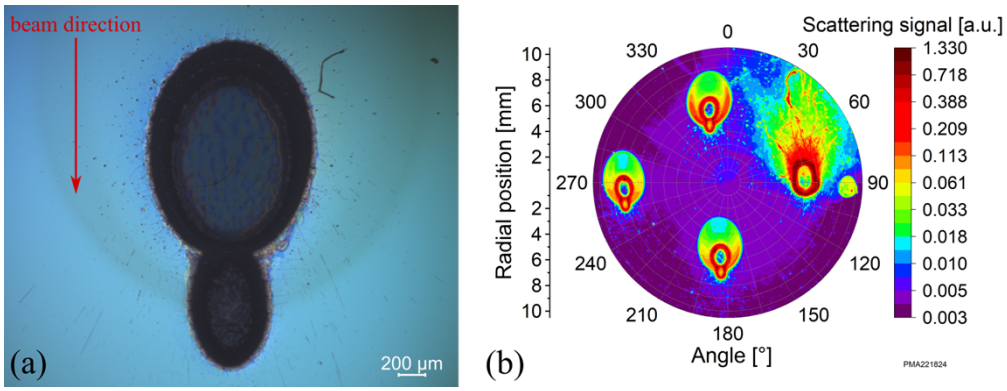

Fig. 6. Microscopy image (a) of one of the damages seen on the scattering map (b) of a dielectric optic showing the impact of the laser-induced damages.

The microscope image on the left shows a damage of 1-2 mm size and small debris particle emitted in the beam direction at the bottom part. In the scatter image on the right side the increased scattering due to the debris is also still visible up to 4-5 mm away from the induced damage. Also, a discolored zone is visible a few millimeters around the laser damage. Overall, these are all changes on or within the optic, which can obviously decrease the LIDT of subsequent spots of a sample under test.

Furthermore, two exemplary images taken by the infrared camera during the measurement are shown in Fig. 7. On the left the optic is not damaged yet and the image on the right shows the heat impact zone after the damage was detected.

In case of a potentially stress induced damage, it is also important to analyze damaged optics regarding their thermally induced stress. For this reason, optics of different batches were investigated using a "StrainMatic M4/100" polarimeter. It was necessary to use a different batch of optics with a different coating design having lower reflectance at the wavelength of the polarimeter, because the reflectance of the previously presented samples was too high at the wavelength range the system operates at. However, the images depicted in Fig. 8 still illustrate the impact of a laser-induced damage on the state of the samples. All optics show a significant change in the stress, which additionally weakens the optic that could potentially lead to a differed

Optical Materials EXPRESS

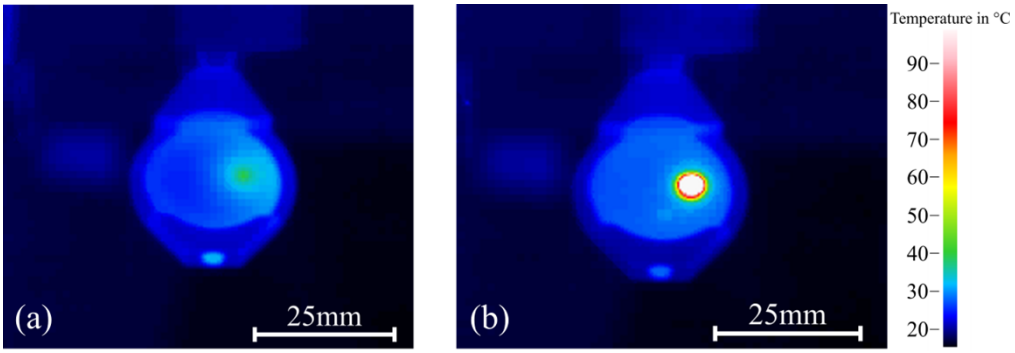

Fig. 7. Image of the infrared camera at the end of an irradiation of 30 s (a) and shortly after the damage was induced within the first second of an irradiation (b).

damage behavior for subsequent damage positions compared to an undamaged component. The optics shown in Fig. 8 are coated with a dielectric multilayer (a) and a hybrid film used in the following section (b) and (c).

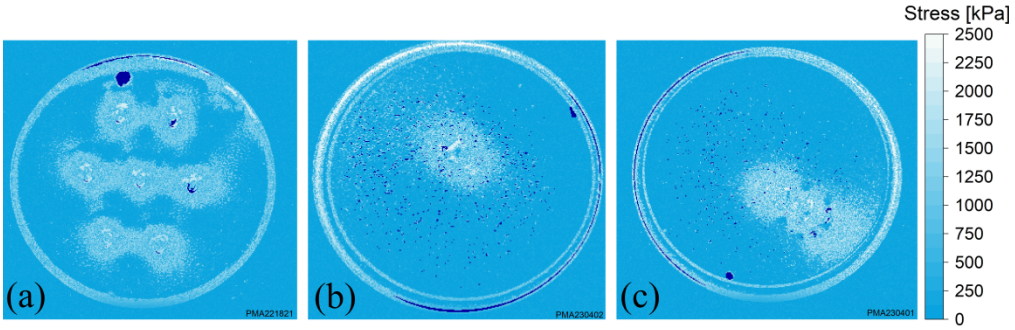

Fig. 8. Stress mapping measured by the polarimeter ‚StrainMatic M4/100“ of a dielectric mirror (a) and of hybrid mirrors (b) and (c) used in the study of the following section.

All the above results show damaged areas of over 1-2 mm and a high contamination on the samples surface due to the laser-induced damages (Fig. 6) and significant induced stresses around the damages (Fig. 8). Moreover, depending on the number of sites and the distance between those sites a noticeable change in the damage behavior can be seen in Fig. 5, leading to the following conclusion: If an optic is damaged during a cw-LIDT test further testing on same sample should not be performed due to unpredictable impact on the subsequent damage behavior.

The previous investigations reveal information on the damage behavior in relation to the morphology of a single test site and the influence of damaged test positions on subsequent interrogations. It is important to note that in the above case we probably observed a defect induced damage mechanism which is also indicated by Fig. 5. As observed in nanosecond and continuous wave [10] LIDT measurements, isolated defects most likely lead to a slight increase in the damage probability in the survival curve. This picture is also in line with the expectations. The absorptivity of dielectric optics is usually so low that even lasers in the multi-kilowatt class cause only small increases in temperature. However, hitting an absorptive defect can lead to a drastic and extremely localized increase in temperature and destroy the sample through stress or melting effects. After the destruction, it is difficult to understand the causes based on the interpretation of the morphology, because the induced modification of the site is relatively big which is why the initial damage mechanisms are not perceptible. Hybrid optics are examined

Optical Materials EXPRESS

in the following section. These usually have higher absorption and are particularly suitable for including the classic models.

5. LIDT of hybrid mirrors with various reflectance and transmittance values

Based on the above observations and interpretation, we investigated hybrid coated mirrors at a wavelength of 1030 nm and an angle of incidence of 45°. The hybrid design consists of an aluminum layer, a MgF_2 cover layer protecting the metal thin film against environmental influences and a dielectric multilayer film ensuring high reflectance at a specific wavelength. These initial two films were deposited by thermal evaporation and the subsequent reflective dielectric Ta_2O_5 - SiO_2 multilayer design was deposited by ion beam sputtering process on top of the sample. A corresponding sketch of the optic is shown in Fig. 9.

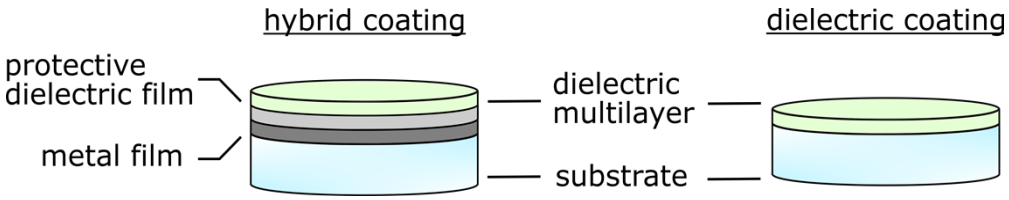

Fig. 9. Sketch of the coated hybrid and pure dielectric mirrors used in this investigation.

The aim of this study was to analyze the impact of optical properties on the LIDT. Due to the thermally driven damage mechanisms the absorption of the metal film in hybrid coated optics was of major interest in this investigation. For this reason, we varied the reflectance of the dielectric multilayer between 90, 99 and 99.9% and the transmittance of the aluminum layer between 0, 16 and 28%. The corresponding aluminum layer thicknesses are approximately 180, 8, and 5 nm determined by a calculated fit using the software OptiRE by OptiLayer [21]. It is important to note that the relative uncertainty of the fitted layer thickness values is estimated to be approximately 20% due to the uncertainty of the material parameters and process stability. By changing the transmittance and reflectance of the dielectric layers, the incident power on the metal film and the total absorption of the film were varied. Moreover, we used fused silica and sapphire substrates to consider the thermal conductivity in this parameter study.

We determined the absorption of the hybrid coated fused silica optics using a laser calorimetry setup [22] with a wavelength of 1064 nm at an angle of 45°. The results are listed in Table 3.

Table 3. Determined absorption in dependence of the dielectric multilayer reflectance and the transmittance of the aluminum and MgF_2 film stack

Transmittance of the aluminum MgF_2 film stack [%]	Reflectance of the Ta_2O_5 - SiO_2 dielectric multilayer film [%]	Measured absorption of the hybrid coating [ppm]	Samples tested regarding LIDT
0	90	13600	3
0	99	8500	2
0	99.9	1550	3
16	99.9	349	3
28	99.9	188	3

In consideration of the results in the previous section we performed 1-on-1 LIDT tests with a nearly centered irradiation on the optic. The optic was irradiated for 30 s, passively cooled down for 90 s, the sample was moved by 400 µm and then the power density was increased. This process was repeated until a damage was induced or the maximum power density was

Optical Materials EXPRESS

reached. In Fig. 10 (a) the highest linear power density the mirrors survived is plotted over the transmittance of the metal film. Each mirror in this graph was coated with a HR dielectric film (99.9% reflectance). In Fig. 10 (b) the highest linear power density the mirrors survived is plotted versus the reflectance of the dielectric coating. The optics in this graph had an aluminum layer with 0% transmittance. The right y-axis shows the percentage of an incident beam which is not absorbed by the optic calculated by subtracting the measured absorption shown in Table 3 from 100%.

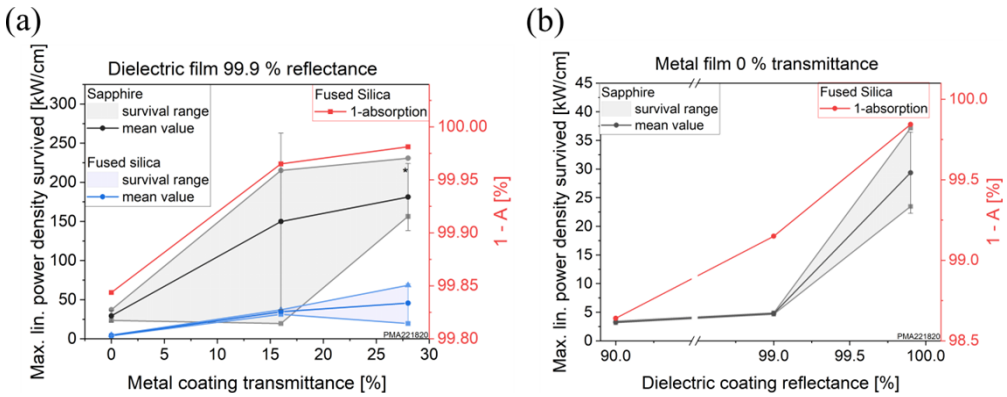

Fig. 10. Maximum linear power density, which the optics survived in dependence on the transmittance of the metal coatings regarding a dielectric coating with 99.9% reflectance (a) and in dependence of the dielectric reflectance regarding a metal film with 0% transmittance (b). (*One HR mirror was not damaged by the highest power output and therefore, the mean value as well as the survival range might be higher)

An increase in the metal layers transmittance i.e., a thinner layer, changes the coating design leading to a higher LIDT due to lower absorption as can be seen in the left image of Fig. 10. If the transmittance is increased from 0% to 16% the relative LIDT increases by a factor of 5 and an increase of the transmittance from 0% to 28% increases the LIDT by at least a factor 6. Regarding this, it is important to note that one of the mirrors with an aluminum layer with 28% transmittance was not damaged thus the mean value and survival range might be higher. Moreover, the impact of the substrates thermal conductivity also becomes visible. Sapphire has a thermal conductivity between 41 W/(m·K) at 0 °C and 20 W/(m·K) at 220 °C [16] whereas Fused Silica has a thermal conductivity between 1.38 W/(m·K) at 20 °C and 1.55 W/(m·K) at 200 °C [17]. The higher thermal conductivity of the sapphire substrate leads to a 4.0 - 6.9 higher LIDT. Our simulations (see Section 2) predicted, in case of a damage behavior governed by the absolute temperature, a difference in the input power by a factor of 7.6 and a damage mechanism driven by the temperature gradient a factor of 1.8. Based on these results the governing damage mechanisms seem to be rather driven by the maximum temperature.

One can see in the right graph in Fig. 10 that an increase in the dielectric film reflectance also increases the LIDT. This is due to a lower incident power on the metal film with higher reflectance. Especially the increase of 99% to 99.9% shows a significant increase in the LIDT from 4.8 kW/cm to 29.4 kW/cm. Interesting to note is also that one of the mirrors with a 99% reflectance coated on a fused silica substrate did not even survive the lowest linear power density used in the setup which is why the fused silica samples are not shown in the graph.

Overall, a significant correlation between the sample absorption and the mean survived linear power densities becomes visible in Fig. 10. To illustrate this more clearly, the mean survived linear power density of the coated sapphire substrates versus the absorption of the coatings is depicted in Fig. 11. It is worth mentioning again that the absorption was measured only for the

Optical Materials EXPRESS

fused silica coated samples, which feature identical coatings. The absorption of the substrates itself can therefore be neglected due to the comparatively low absorption below 20 ppm for both materials.

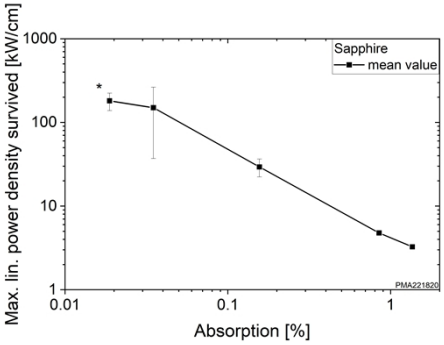

Fig. 11. The maximum linear power density, which the mirrors survived, versus the absorption of the surface coating. (*One HR mirror did not get damaged at the highest power output therefore the mean value might be higher)

6. Conclusion

The investigation was designed to measure the damage behavior of optical components for high continuous powers. Initially, it was found that the measurement protocols developed and used so far for the investigation of the laser induced damage thresholds did not provide valid results. The reason for this was identified as severe damage to non-irradiated areas of the sample due to the extensive and big heat input. This effect drastically limits the number of measurement positions on the specimen, which reduces the statistical reliability of the measurement. In order to obtain reproducible and meaningful measurement results despite the obvious physical problem, a protocol was chosen that is based on a continuous increase of the power densities. To exclude conditioning and fatigue effects, a new position in the optics center with a displacement of a few hundred micrometers was selected for each irradiation. In case of the occurrence of a laser-induced damage, the sample was not irradiated any further. This provided the necessary certainty for the measurement also for 25 mm samples. Obviously, a large quantity of samples needs to be chosen to reliably determine the damage threshold for the study leading to very time-consuming measurement protocols. For large-sized specimens, several damaged positions could be used, but it must be ensured that debris and stresses of the destroyed position do not influence one of the subsequent positions, which is difficult to realize in practice.

For this study, dielectric optics and hybrid optics made of a metal thin film and a dielectric film were investigated. For the dielectric optics, the influence of inhomogeneities and defects seems to dominate. For hybrid optics, clear correlations to absorptive damage could be established. It could be shown that the metal layer is significantly responsible for the damage. The less the metal layer absorbs, the higher the LIDT of the entire component. The same applies if the metal layer is shielded by a dielectric layer stack. The higher the reflectivity of the layer stack, the higher the LIDT. Furthermore, it was shown that the choice of a suitable substrate material can significantly improve the damage threshold. The same coatings on sapphire substrates showed a damage threshold up to 7 times higher than the comparison coating on fused silica, which qualitatively confirms the simulation results. For future studies, the influence of heat dissipation should be given even greater importance.

Disclosures. The authors declare no conflict of interest.

Optical Materials EXPRESS

Data availability. Data underlying the results presented in this paper are not publicly available at this time but may be obtained from the authors upon reasonable request.

References

1. A. Mahrle and E. Beyer, "Theoretical aspects of fibre laser cutting," J. Phys. D: Appl. Phys. **42**(17), 175507 (2009).
2. A. Hess, R. Schuster, A. Heider, R. Weber, and T. Graf, "Continuous Wave Laser Welding of Copper with Combined Beams at Wavelengths of 1030 nm and of 515 nm," Phys. Procedia **12**, 88–94 (2011).
3. S. Katayama, *Handbook of Laser Welding Technologies*, Woodhead Publishing, (2013).
4. S. Grabmann, J. Kriegler, F. Harst, F. J. Günter, and M. F. Zaeh, ",Laser welding of current collector foil stacks in battery production-mechanical properties of joints welded with a green high-power disk laser," Int J Adv Manuf Technol **118**(7-8), 2571–2586 (2022).
5. P. A. Rometsch, Y. Zhu, X. Wu, and A. Huang, ",Review of high-strength aluminium alloys for additive manufacturing by laser powder bed fusion," Mater. Des **219**, 110779 (2022).
6. P. von Jan and M. Axtner, ",Mirror technology is the key," Laser Tech. J. **8**(3), 20–23 (2011).
7. J. Hue, J. DiJon, and P. Lyan, "Thermal behavior of optical mirrors under high-power continuous wave CO2 laser irradiation", Proc. SPIE 1848, (1992).
8. H. Gong, C. F. Li, and Z. Y. Li, "CW-laser-induced thermal and mechanical damage in optical materials", Proc. SPIE 3578, (1998).
9. R. M. Wood, *Laser-induced damage of optical materials*, CRC Press, (2003).
10. A. Brown, D. Bernot, A. Ogloza, K. Olson, J. Thomas, and J. Talghader, "Physical Origin of Early Failure for Contaminated Optics," Sci. Rep. **9**(1), 635 (2019).
11. L. Lamaignére, A. Ollé, M. Chorel, N. Roquin, A. A. Kozlov, B. N. Hoffman, J. B. Oliver, S. G. Demos, L. Gallais, R. A. Negres, and A. Melninkaitis, "Round-robin measurements of the laser-induced damage threshold with sub-picosecond pulses on optical single layers," Opt. Eng. **60**(03), 031005 (2020).
12. D. Ristau, *Laser Damage in Optical Materials*, (CRC Press, 2014), p. 18–20.
13. COMSOL, [Online]. Available: https://www.comsol.de/heat-transfer-module. [Accessed 20 10 2022].
14. D. A. Ditmars, S. Ishihara, S. S. Chang, and G. Bernstein, "Enthalpy and Heat-Capacity Standard Reference Material: Synthetic Sapphire (α-$A1_20_3$) from 10 to 2250 K," Journal of Research 87(2), (1982).
15. TA Instruments, [Online]. Available: https://www.tainstruments.com/pdf/literature/TN8.pdf. [Accessed 25 10 2022].
16. SHINKOSHA Co., Ltd., [Online]. Available: https://www.shinkosha.com/english/techinfo/feature/. [Accessed 20 10 2022].
17. Heraeus Group, [Online]. Available: https://www.heraeus.com/media/media/hca/doc_hca/products_and_solutions_8/optics/Daten_und_Eigenschaften_Quarzglas_fuer_die_Optik_DE.pdf. [Accessed 20 10 2022].
18. R. A. Negres and C. J. Stolz, "1077-nm, CW mirror thin film damage competition," SPIE Laser Damage, (2022).
19. S. Schrameyer, M. Jupé, L. O. Jensen, and D. Ristau, "Algorithm for cumulative damage probability calculations in S-on-1 laser damage testing," Proc. SPIE **8885**, 88851J (2013).
20. P. Kadkhoda, W. Sakiew, S. Günster, and D. Ristau, "Fast total scattering facility for 2D inspection of optical and functional surfaces," Proc. SPIE **7389**, 73890S (2009).
21. OptiLayer. [Online]. Available: https://www.optilayer.com/products-and-services/optire [Accessed 02.12.2022].
22. U. Willamowski, D. Ristau, and E. Welsch, "Measuring the absolute absorptance of optical laser components," Appl. Opt. **37**(36), 8362–8370 (1998).